Journal of Molecular Structure 1276 (2023) 134761

Contents lists available at ScienceDirect

Journal of Molecular Structure

journal homepage: www.elsevier.com/locate/molstr

Equilibrium and DFT modeling studies for the biosorption of Safranin O dye from water samples using *Bacillus subtilis* biosorbent

Serap Çetinkaya[a,*], Savaş Kaya[b], Aysun Aksu[a], Halil İbrahim Çetintaş[c], Nida Shams Jalbani[d], Sultan Erkan[b], Riadh Marzouki[e,f]

[a] Sivas Cumhuriyet University, Science Faculty, Department of Molecular Biology and Genetics, 58140 Sivas, Turkey
[b] Department of Chemistry, Faculty of Science, Sivas Cumhuriyet University, Sivas 58140, Turkey
[c] Advanced Technology Research and Application Center (CUTAM), Sivas Cumhuriyet University, 58140 Sivas, Turkey
[d] National Center of Excellence in Analytical Chemistry, University of Sindh, Jamshoro 76080, Pakistan
[e] Chemistry Department, College of Science, King Khalid University, Abha 61413, Saudi Arabia
[f] Chemistry Department, Faculty of Sciences of Sfax, University of Sfax 3038, Tunisia

ARTICLE INFO

Article history:
Received 5 November 2022
Revised 2 December 2022
Accepted 6 December 2022
Available online 7 December 2022

Keywords:
Biosorption
Equilibrium modes
Kinetic modeling
Molecular docking
Safranin O dye
Thermodynamic study

ABSTRACT

Current study deals with the biosorption of Safranin O dye from water by using high potential *Bacillus subtilis* biosorbent material. The presence of functional groups and surface morphology of biosorbent was analyzed by using sophisticated analytical techniques such as FT-IR (Fouirer Transform Infrared Spectrophotometer), SEM (Scanning Electron Microscopy), EDX (Energy Dispersive X-Ray Analysis), and TGA (Thermogravimetric Analysis). To check the dye removal potential of *Bacillus subtilis* sorbent, batch adsorption experiments were performed under the optimized conditions. The biosorption experiments showed that the *Bacillus subtilis* sorbents remove 80% of safranin O dye from water. The biosorption mechanism is depends upon the solution pH thus the maximum biosorption was observed at (5.5–6.5). Moreover, the biosorbent dose has been optimized and it has observed that the maximum concentration of safranin O dye has been removed using the 50 $mg.L^{-1}$ of *Bacillus subtilis*. The biosorption equilibrium data were well fitted by the Langmuir adsorption isotherm due to good regression coefficient value (R^2=0.98) and better Langmuir capacity (0.383 $mmol.g^{-1}$), while the kinetic studies indicated that the biosorption followed the pseudo-second-order model. The thermodynamic parameters values showed that the biosorption is process is endothermic and spontaneous nature. In addition, molecular docking was also performed to examine the interaction between the safranin O dye molecule and the *Bacillus subtilis* bacterial cell line.

1. Introduction

Treatment of dye contaminated water in industrial outlets is an ever growing problem which demands innovative technological solutions [1]. They are characterized by high alkalinity, high biological- and chemical oxidation demands, and high solid content [2,3]. Furthermore, synthetic-aromatic dyes are highly recalcitrant to biological degradation [4,5].

Dye contaminants in wastewater are generally removed by physical or chemical treatment processes. These include electroflocculation, membrane filtration, flotation, ion exchange chromatography, electro-kinetic coagulation, electrochemical degradation, ozonation, precipitation, irradiation, and catox purification, involving the use of mixtures of activated carbon and air. However, these technologies are generally ineffective in sufficient decoloration, relatively expensive, and less adaptable to novel problems [5,6].

Biological adsorption (biosorption) methods to eliminate dyes, efficiency, cost-effectiveness, low maintenance, etc. It is advantageous in terms of today's physical and chemical techniques. Simplicity and low cost make adsorption a systematic method for dye removal from aqueous solutions. Changing the surface chemistry of adsorbents usually improves adsorption [7,8].

Biosorption is also a promising technology both in the removal and in the recovery of heavy- and precious-metal contaminants [9]. Biomasses of, bacteria, fungi, sludge, algae, yeast, and by-products of agricultural industry have recently been exploited as the sources of biosorbent [10]. Biosorption of ionic pollutants usually takes place through the functional groups on the biomass surface [11].

The biosorption properties of bacterial biomass have been well documented [12,13]. It often occurs via electrostatic forces as well

* Corresponding author.
E-mail address: serapcetinkaya2012@gmail.com (S. Çetinkaya).

https://doi.org/10.1016/j.molstruc.2022.134761
0022-2860/

as covalent bonding. The most important component of microbial biosorbent appears to be the cell wall and bacteria has two main types: Gram-positive and Gram-negative. Here two anionic functional groups in the thick peptidoglycan and in teichoic acids play the crucial role in the binding of metal ions [11,14]. The mode of uptake of solutes by dead/inactive cells is therefore extracellular [5,15].

Bacillus subtilis is one of the bona fide source of biosorbent compounds. The structure of its cell wall is well known and consists mainly of teichoic acid and peptidoglycans. Teichoic acid is a bacterial copolymer of glycerol phosphate or ribitol phosphate, mainly exposing phosphate and hydroxyl groups. Peptidoglycan, also known as murein, is a polymer composed mainly of N-acetylmuramic and N-acetylglucosamine acids that exhibit carboxylic and hydroxyl functional groups [16,17].

Safranin (3, 7-diamino-2, 8-dimethyl-5-phenylphenazine-5-ium chloride) is the known oldest water-soluble synthetic dye. It is generally used for dyeing cotton, fibers, leather, paper, silk, tannin, and wool. It is also widely used as a colorant in the food and textile industries [18].

In this study, the biosorption of safranin O dye on the biomass of *Bacillus subtilis* was investigated. *Bacillus subtilis* has high physiological activity as the biosorbent material. *Bacillus* members are widely distributed in the nature. The biosorption of safranin at solid/liquid interfaces was studied under the equilibrium conditions. Factors influencing the biosorption, namely, temperature, initial pH of the dye solution, and biosorbent concentration, were investigated. Finally, kinetics of the biosorption was assessed.

2. Materials and methods

2.1. Isolation and identification of Bacillus subtilis

The isolate was found in orchard soil samples (Çamlıbel, Tokat, Turkey). Isolation was carried out as described [19] and stored [20]. Identification was based on the V3-V4 variable region sequence of 16S rRNA gene. Genomic DNA was extracted and used as the template [21,22]. Sequence information was obtained in the Illumina MiSeq at Sivas Cumhuriyet University Advanced Technology Research and Application Center (CUTAM) and stored in GenBank (Accession number: OM146541). The isolate was identified using BLAST [23]. The sequence was then analyzed by MAFFT program [24] and a phylogenetic tree was built using the Kimura-2 genetic distance model and Neighbour-joining (NG) method [25,26] (Fig. 1). The tree topology was tested for 500 times by Bootstrap method.

2.2. Preparation of the biosorbent

A bacterial culture, 150 mL, was obtained in a 250 mL flask, by incubation for 24 h at 37 °C at 150 rpm and. The cells were pelleted by centrifugation for 10 min at 5000 rpm (Eppendorf 128 5804, Germany). The cells were weighed after drying for 24 h at 105 °C.

2.3. Batch biosorption experiments

Stock solution of 1000 ppm of Safranin O dye was prepared in deionized water. All the biosorption experiments were carried out 25 °°C by shaking 50 mg of biosorbent in 50 mL dye solution and equilibrated for 60 min to ensure proper agitation. The solution pH was adjusted (2, 3, 4, 5, 6, 7, 8, 9, 10, 11, 12) using 0.01 M solution of HCl/NaOH. The pH experiments were studied by shaking 50 mg biosorbent in 50 mL of dye solution at different pH and 25°C for 60 min. Isothermal and kinetic studies were conducted at 25 °C, whereby 50 mg of biosorbent was kept in contact with 50 mL of dye solution of varying concentrations (10–250 mg/L) at different time intervals (5–140 min) at pH 5.5. The biosorbent from the solution mixture was separated by centrifugation at predetermined time-intervals [27]. Then remaining dye concentration in the solution was analyzed by using UV–Visible spectrophotometer at 530 nm. The adsorption percentages and adsorption capacities were calculated using the Eqs. (1) and 2.

$$\%\ Adsorption = \frac{C_i - C_f}{C_i} \times 100 \quad (1)$$

$$q_e = \frac{(C_i - C_e)V}{m} \quad (2)$$

Where C_i and C_f are the initial and final concentrations, C_e is the equilibrium concentration of Safranin O dye.

2.4. Computational detail

Docking Server was preferred as the docking calculation program. Safranin has been optimized in MMFF94 in the server. The load calculation method was chosen as Gasteiger. pH = 7.0 was taken for all calculations. In docking calculations, grid maps 90 × 90 × 90 Å (x, y and z) and Lamarckian genetic algorithm (LGA) and Solis & amp; wet local search method was used. The population size was set to 150. A translation step of 0.2 Å and a 5 Å quaternion and torsion steps were applied during the search for the appropriate region of the target protein of the molecules studied [28]. Application of the PM6 semi-empirical method to modeling proteins enhances docking accuracy of AutoDock. A semi empirical free energy force field with charge-based desolvation [29].

3. Results and discussion

3.1. Characterization of biosorbent

3.1.1. FT-IR study

Fourier transform infrared (FTIR) technique plays an important role to investigate the interaction between the surface of the adsorbent and the dye by identifying the characteristic adsorption bands of the materials [30]. The FTIR spectra of *Bacillus subtilis* and Safranin O dye were studied within the range of 400–4000 cm^{-1} and were shown in Fig. 2. As shown in the FTIR spectrum of *Bacillus subtilis*, amide A band, one of the characteristic bands of proteins, was observed at 3271 cm^{-1} [31]. The peak at 2927 cm^{-1} was attributed to CH_2 asymmetric stretching of acyl chains of lipids [32]. The peaks centered at 1634 cm^{-1} and 1538 cm^{-1} were assigned to amide I and amide II bands which were two major peaks of the protein infrared spectrum [31]. The adsorption band at 1396 cm^{-1} corresponded to COO^- symmetric stretching vibration of amino acids [33]. The peaks located at 1232 cm^{-1} and 1057 cm^{-1} were assigned respectively to asymmetric and symmetric stretching of PO_2^- stemmed from C–O–P stretching of proteins and lipids [34]. After exposing the *Bacillus subtilis* with Safranin O, new adsorption bands occurred. The peak that appeared at 3196 cm^{-1} was generated by the N-H group which confirmed the interaction between the dye and cell wall of the bacteria [35]. The peaks centered at 1641 cm^{-1}, 1611 cm^{-1}, 1529 cm^{-1} and 1493 cm^{-1} were the result of the C=C stretching vibrations which could support the presence of an aromatic structure [36,37]. Also, C–N stretching of aromatic tertiary amine was observed at 1328 cm^{-1} [36]. From the result of FTIR analysis, it was concluded that the Safranin O molecules were biosorbed on the surface of *Bacillus subtilis* by interacting with carboxyl and hydroxyl groups presented on the cell wall of bacteria [38].

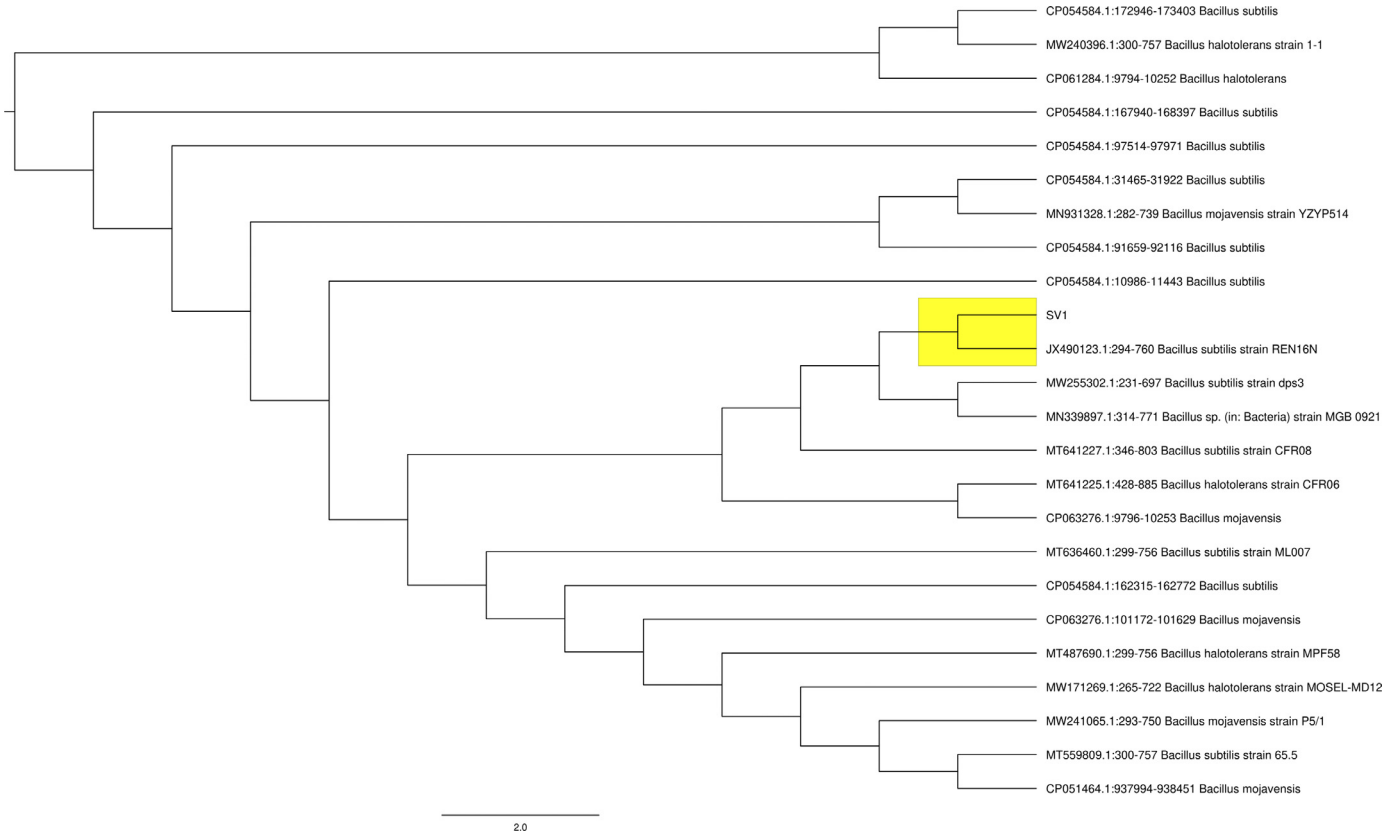

Fig. 1. Dendrogram of *Bacillus subtilis* strains and SV1 isolate.

3.1.2. SEM-EDX analysis

SEM images of the bacterial cell surface before and after the biosorption process of Safranin O dye at 20 kx were shown in Figs. 3(a and c). Before treatment, agglomerated bacterial cells were rod-shaped and had smooth surfaces [39]. However, the morphology of dye-treated cells changed significantly and the cell surfaces became rough, uneven and spongy [40]. The morphological changes were attributed to the Safranin O dye which interacted with the functional groups, responsible for the biosorption, of the cell surface and deposited onto biomass [8]. These findings agreed with the information provided by the EDX analysis which is a useful examination to determine the elemental characteristics of biosorbent. The results obtained from EDX showed that the elemental composition changed after biosorption process Figs. 3(b and d). The content of C and Cl^- (wt%) increased from 59.28 and 1.10 to 62.03 and 2.23 respectively due to the presence of chlorine ions and the high carbon content of the dye. This analysis confirmed that the Safranin O dye was biosorbed on the cell surfaces of *Bacillus subtilis*.

3.1.3. TGA analysis

The TGA has been performed to check the thermal stability of biosorbent (Fig. 4). TGA analysis demonstrates that the thermal degradation of biosorbent takes place in two steps; first step is from 60 to 200 °C with (10%) loss of adsorbed water molecules while the organic material of biosorbent show weight loss of (above 60%) at temperature 200 °C to 600 °C. The major losses have been noticed at 300 to 500 °C that was due to the combustion of biosorbent organic material and functional groups. In literature, many researchers used TGA to examine the thermal stability of biosorbent such as orange peel waste biosorbent were previously applied for the water treatment and characterized by TGA techniques. Similarly another researcher characterized *Bacillus subtilis* biosorbent using TGA technique and applied for the removal of MB (methylene blue) dye from water.

3.1.4. XRD characterization of biosorbent material

X-ray diffraction analysis (XRD) is a most common analytical technique used in the field of science and technology to characterize the crystallographic structure of a material. This techniques is based on by irradiating a solid material/sorbent with incident X-rays and then measuring the intensities and scattering angles of the X-rays that leave the material/adsorbent and the materials are identified on their diffraction pattern. In sorption phenomenon, sorbent materials are made up of regular arrays of atoms/particles, and these particles scatter incident X-rays, through their interaction. Herein, the biosorbent material has been characterized by XRD technique Fig. 5a, which shows that material has less crystallinity and has some angles at (24.3, 33.2, 42.2 and 48.6), which shows that biosorbent is amorphous in nature. Due to less crystallinity and amorphous nature of biosorbent, it shows high adsorption capacity for the sorption of safranin O dye (Fig. 5b).

3.2. Effect of *pH*

Fig. 4 demonstrates the effect of pH on the biosorption of Safranin O dye at the equilibrium condition using *Bacillus subtilis* biosorbent material. It is clear in Fig. 6 that the percentage of biosorption was maximum at pH 5.5. At higher acidic medium, the biosorbent surface has been protonated which effect the binding cites of biosorbent while at basic medium, the amine groups of dye molecules are deprotonated, and produced electrostatic repulsion forces between biosorbent and dye molecules. Thus, the opti-

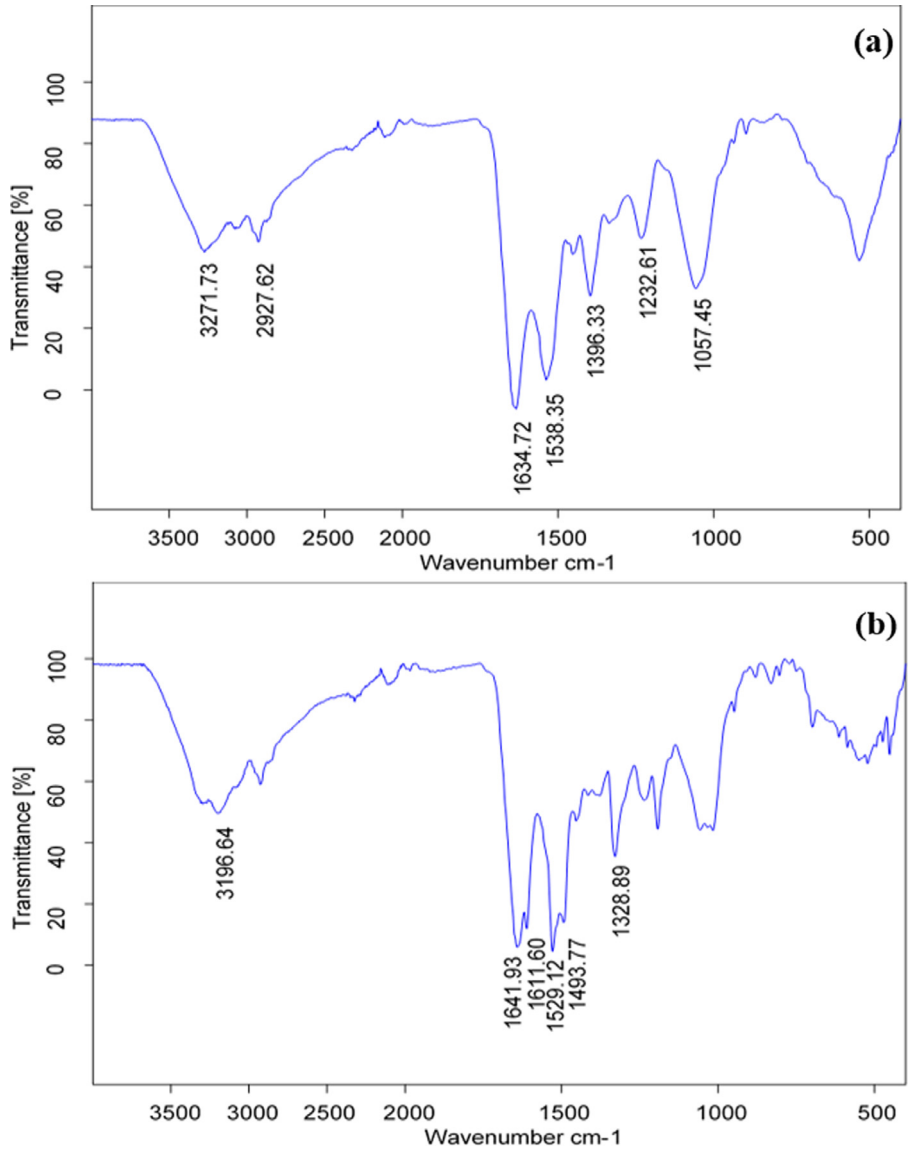

Fig. 2. FT-IR spectra of *Bacillus subtilis* before (a) and after (b) the biosorption process of Safranin O dye.

mized pH was 5.6 and other experiments were carried out at this pH.

3.3. Effect of biosorbent dosage

The effect of *Bacillus subtilis* dosage on the biosorption of safranin O dye was investigated and it has been found that the% adsorption is increased as the dosage increased up to 50 mg.L^{-1} as shown in Fig. 7. The addition of further higher doses has no significant effect on adsorption percentages due to almost saturation of binding sites of *Bacillus subtilis* biosorbent, thus, the adsorption capacities (g.mol^{-1}) were decreased.

3.4. Isotherm models

The biosorption equilibrium models play an important role in the adsorbate-adsorbent interaction phenomenon. The Langmuir isotherm model is most commonly used to explore the monolayer adsorption of a solute onto solid surface and it also calculate the maximum uptake values of adsorbate. Mathematically Langmuir model can be calculated using following Eq. (3) while the essential characteristics of the Langmuir model can be calculated by using Eq. (4).

$$\left(\frac{C_e}{C_{ads}}\right) = \left(\frac{1}{Qb}\right) + \left(\frac{C_e}{Q}\right) \tag{3}$$

$$R_L = \frac{1}{(1 + bC_i)} \tag{4}$$

Where Q (mol.g^{-1}) is the Langmuir uptake capacity, b (L.mol^{-1}) is the Langmuir constant, Ce is the equilibrium concentration. Thus, the Langmuir model has been applied on biosorption data, and it was observed that the equilibrium data of Safranin O dye was best-fitted by the Langmuir equation with good correlation coefficient (R^2=0.98) (Fig. 8) as well high Langmuir biosorption capacity (0.33 mol.g^{-1}) (Table 1). The R_L parameter values of Langmuir describe the nature of biosorption process (irreversible R_L=0, favorable $0 < R_L < 1$, linear R_L 1 or unfavorable $R_L > 1$). Herein, R_L ranged from 0.5–0.95 (Table 1) for the biosorption of Safranin O dye which confirming the favorable biosorption process by *Bacillus subtilis* biosorbent.

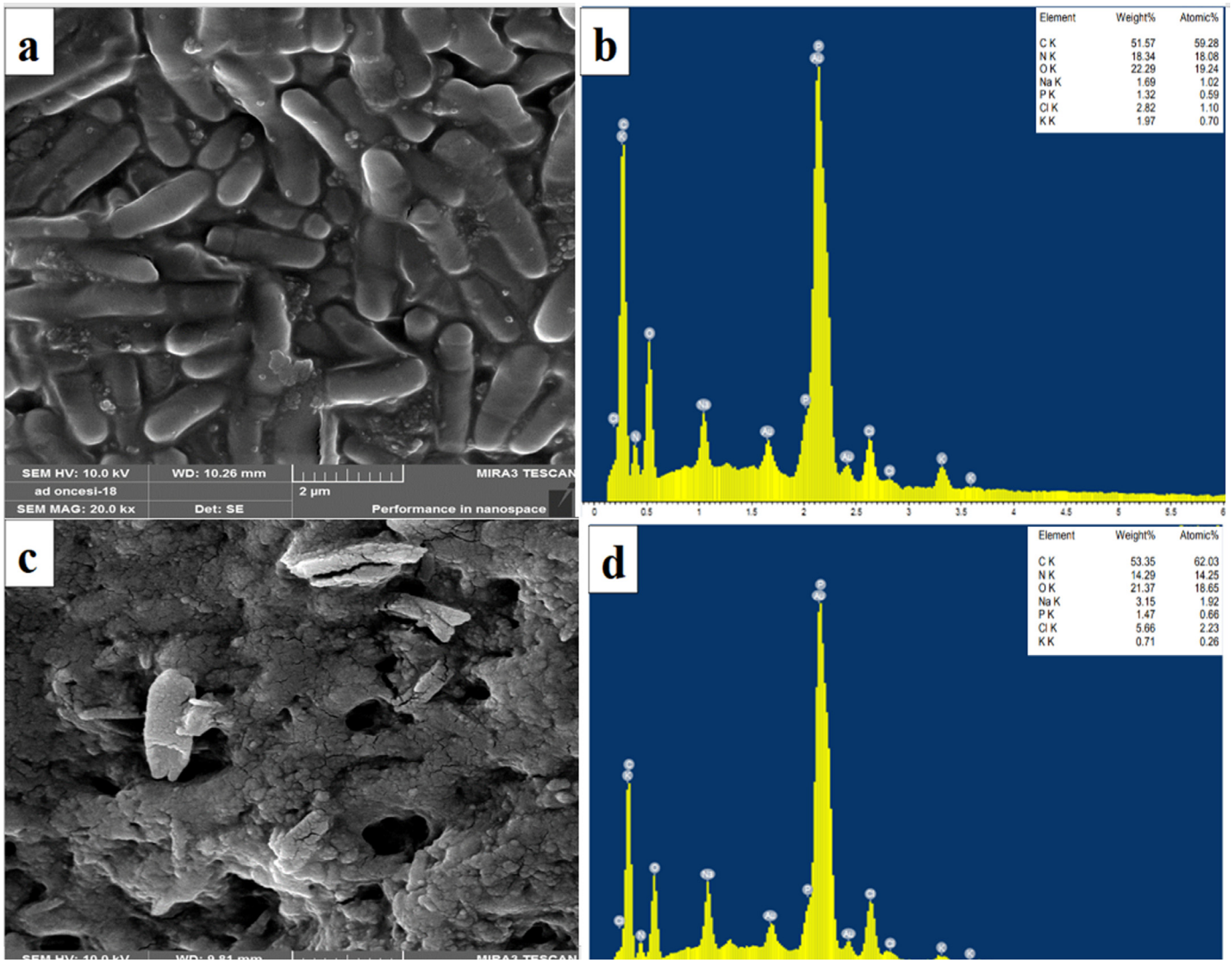

Fig. 3. SEM-EDX images of *Bacillus subtilis* before (a, b) and after (c, d) the biosorption process of Safranin O dye.

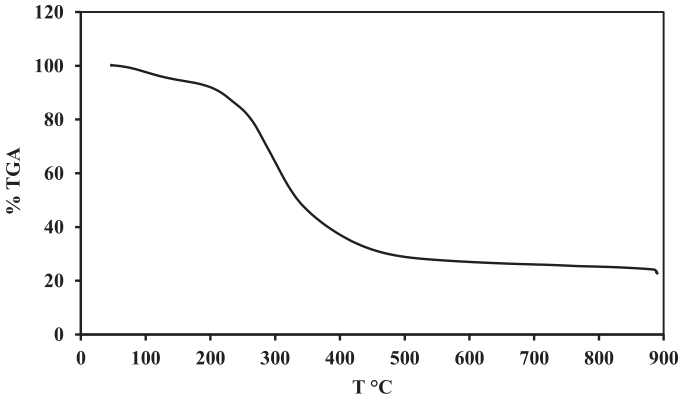

Fig. 4. Thermogravimtric curve of biosorbent.

The Freundlich biosorption equilibrium model explains the reversible and heterogeneous multilayer surface formation. Herein, the biosorption equilibrium data was subjected towards the Langmuir model by using equation 5. Therefore, the graph has been plotted between the logC_e vs log*Cads* (Fig. 8), from the slop and intercept the constant values (*A* and *1/n*) were calculated (Table 1).

Table 1
The Langmuir, Freundlich and D-R equilibrium models constant values for the adsorption of Safranin O dye from water using bio-sorbent.

Parameters	Langmuir	Freundlich	D-R
Q (mmol.g^{-1})	0.383	_	_
b	48.28	_	_
R_L	0.5–0.95	_	_
A(mol.g^{-1})	_	141.2	_
1/n	_	0.659	_
n	_	1.517	_
Xm (mol.g-1)	_	_	0.00193
E(KJ/mol)	_	_	9.533
R^2	0.9834	0.971	0.920

According to the data of the fitted models, Langmuir model fits slightly better with better correlation coefficients compared with Freundlich isotherm, indicating the process to correspond to monolayer adsorption. Generally, as the (*A*) value decreases the biosorption capacity of the biosorbent-material is decreased, while the 1/n values suggest less importance of heterogeneity in the biosorption phenomenon.

$$\log C_{ads} = \log A + \left(\frac{1}{n}\right) \log C_e \tag{5}$$

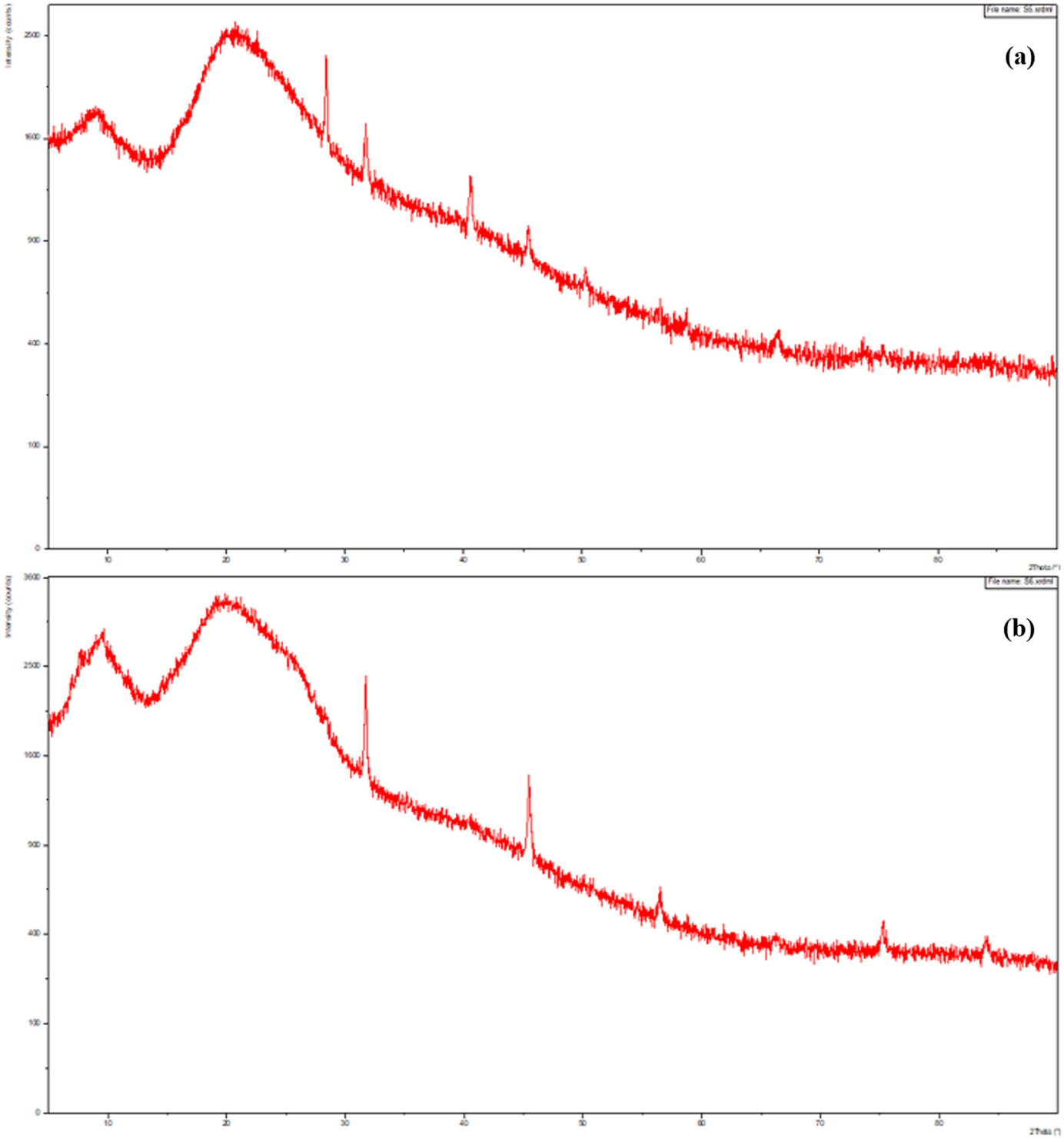

Fig. 5. XRD curves before (a) and after (b) biosorption.

The D–R biosorption isotherm model is helpful to discriminate the physical/chemical biosorption process. Thus the graph has been plotted between (ε) vs *lnCads* (mol.g^{-1}) (Fig. 8) by utilizing Eq. (6).

$$\ln C_{ads} = \ln X_m - \beta\varepsilon^2 \quad (6)$$

Based on the D-R model results (Table 1), t (Xm= 0.00193 mol.g^{-1}, E = 9.533 KJ.mol^{-1}) suggested that the biosorption phenomenon is chemisorption in nature.

3.5. Kinetic study

The biosorption is time dependent process, thus the rate determining steps must be known to validate the equilibrium mechanism. In dyes contaminated water treatments, kinetic study is very important to highlight the kinetic reaction mechanism of biosorbent and adsorbate. Herein, the two kinetic models such as pseudo first order (PFO) and pseudo second order (PSO) kinetic models

Table 2
Pseudo first and second order kinetic models constant values for the adsorption of Safranin O dye from water using bio-sorbent.

Pseudo First Order				Pseudo Second Order		
Erythrosine B	K_1(min^{-1})	qe (mol/g)	R^2	K_2 (min^{-1})	qe (g/mol.min^{-1})	R^2
	1.50	1.01	0.9644	0.0661	1.7101	0.9738

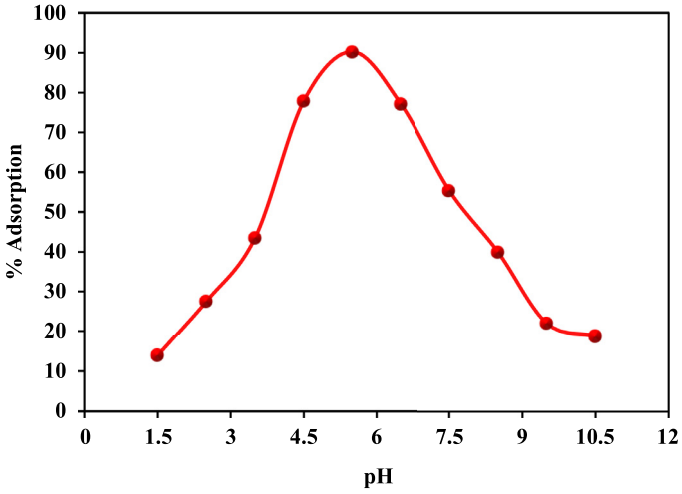

Fig. 6. Effect of pH on the adsorption of safranin O dye from water using *Bacillus subtilis* biosorbent.

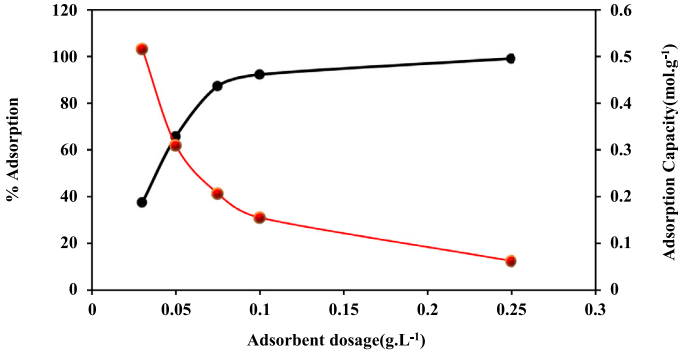

Fig. 7. Effect of biosorbent dosage on adsorption of Safranin O dye from water.

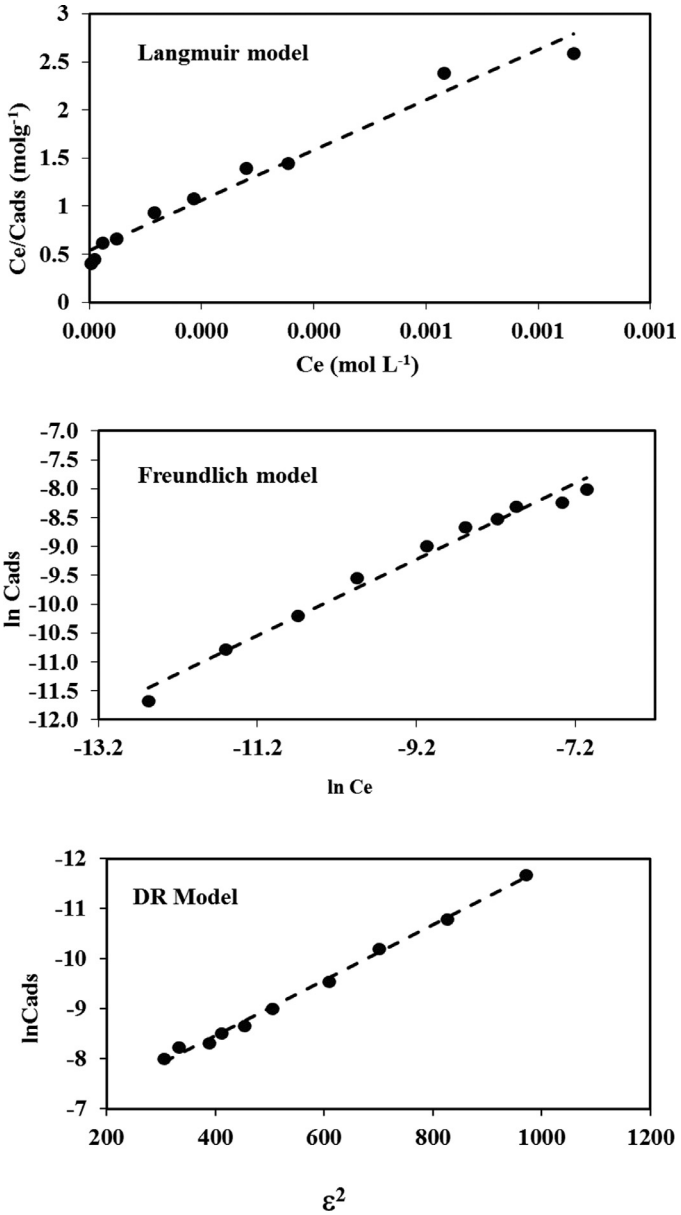

Fig. 8. Langmuir, Freundlich and D-R equilibrium models for the adsorption of Safranin O dye from water using biosorbent.

were applied by utilizing Eqs. (7) and (8) respectively.

$$\ln(q_e - q_t) = \ln q_e - k_1 t \tag{7}$$

$$\frac{t}{q_t} = \left(\frac{t}{k_2 q_e^2}\right) + \left(\frac{1}{q_e}\right) \tag{8}$$

Where, qt is the adsorbed amount of dye (mol.g^{-1}) and (k_1/min) is the 1st order rate constant, while the (k_2) is the rate constant of pseudo second order kinetic model. The equilibrium biosorption data have been exploited using kinetic biosorption models by plotting the graph between ln(q_e-q_t) vs t min (Fig. 9), from the slop and intercept, the PFO kinetic constant parameters were calculated (Table 2). For PSO kinetic model, the graph has been plotted t/qt vs t min (Fig. 9), from the slop and intercept of linear plot, the PSO kinetic values were calculated (Table 2). By comparing the constant values of both models, it is clear that biosorption of Safranin O dye takes place by PSO kinetic model rather than the PFO kinetic model. These results showed that the R^2 value of PSO is 0.9783, while the PFO is 0.964 respectively, which clearly demonstrate that the pseudo-second-order kinetic model is best fit model for the biosorption of Safranin O dye from water.

Table 3
Thermodynamic parameters for the adsorption of Safranin O dye from water using bio-sorbent.

ΔH (KJ/mol)	ΔS(KJ/mol)	ΔG(KJ/mol)		
		293 K	**298 K**	**308 K**
0.0727	**0.0221**	−0.04 *lnKc*= 0.01	−1.22 *lnKc*= 0.5	−1.50 *lnKc*= 0.6

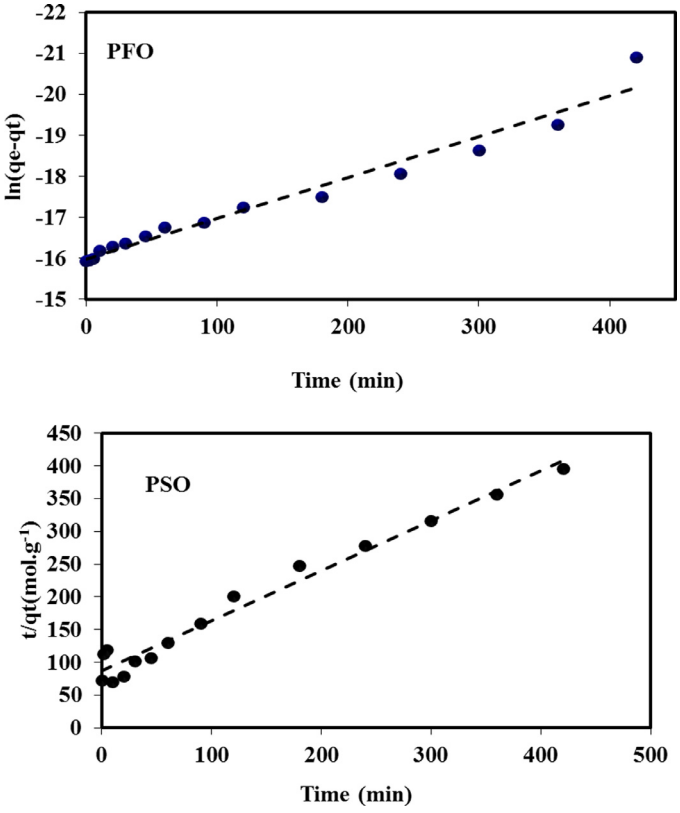

Fig. 9. Pseudo first and second order kinetic models for the adsorption of Safranin O dye from water using biosorbent.

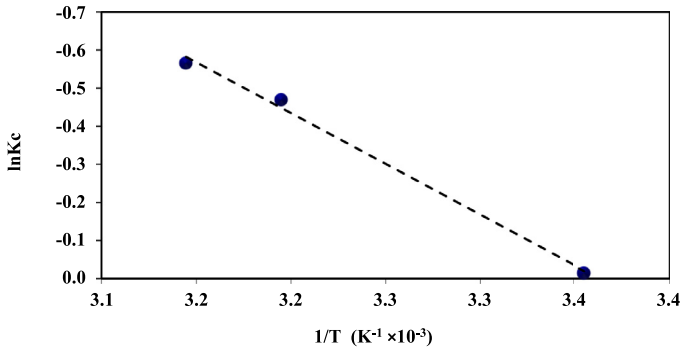

Fig. 10. Effect of temperature on the adsorption of Safranin O dye from water using biosorbent.

3.6. Thermodynamic biosorption study

The thermodynamic study was performed to calculate the (ΔH) change in enthalpy, (ΔS) entropy, and (ΔG) Gibbs free energy at temperature (293, 298 and 308 K). The thermodynamic parameters (ΔH, ΔS, and ΔG) (Table 3) have been calculated from the slope and intercept of the linear plot of lnkc vs 1/T (Fig. 10) using the following Eqs. (9) and (10).

$$\ln k_c = \frac{-\Delta H}{RT} + \frac{\Delta S}{R} \tag{9}$$

$$\Delta G = -RT \ln k_c \tag{10}$$

Where *kc* is equilibrium constant. The feasibility of the biosorption process is proved from the negative values of (ΔG), and endothermic due to positive value of (ΔH). Moreover, the positive value of ΔS indicates that randomness is increased at biosorbent surface.

3.7. Computational study

Molecular docking is of great importance in cell biology, as it is done by interacting a target protein (cell line) with a ligand molecule. It is a key step in drug development. The docking results can be used to find the inhibitor of the target protein and thus new drugs can be developed [41]. *Bacillus subtilis* with simple genetic modification is among the most studied species due to its natural ability for extracellular DNA uptake, which facilitates sporulation formation. PDB ID: 1QD9 was selected from the *Bacillus subtilis* bacterial strain protein database. There is a deep and narrow cleft between the subunits covered with nine side chains that are invariant among 25 similar homologs in *Bacillus subtilis*. This conserved site is suggested to be a binding or catalytic site for a ligand or substrate of the protein family. Docking scores, docking poses and interaction types of Safranin against *Bacillus subtilis* (PDB ID: 1QD9) bacterial line cell are given in Fig. 11.

As seen from Fig. 11, Safranin ligand strongly interacts with the 1QD9 target protein. Safranin molecule formed H-bond with nitrogen atoms and amino acid residues GLU69, GLN93, TYR94 and ASP96. It interacts polar with GLU69 and ASP96 and pi-pi with TYR94. The H-bond indicates strong interaction between Safranin and the 1QD9 target protein. To predict its antibacterial activity, the binding energy (BE), intermolecular energy (IE), van der Waals H-bond desolve energy (WHDE), interaction surface (IS) and inhibition constant (Ki) between ligand-target protein were calculated and Fig. 9 was also given. As seen from Fig. 9, BE, IE, and WHDE values between ligand and target protein are negatively high. These energies are components of the interaction energies between the ligand and the target protein. More negative interaction energy indicates higher inhibition efficiency. According to these energies, they can be the active candidate molecule for bacterial cells of the investigated molecule. On the other hand, a high interaction surface (IS) increases the ligand-protein interaction and causes an increase in antibacterial activity. The inhibition constant (Ki) is a data about the amount of drug to be used in the treatment. The smaller this value, the smaller the amount of drug used in the treatment. The Ki values obtained from the interaction of the studied ligand with the target protein are quite small. This result shows that the ligand can be active even at very low concentrations.

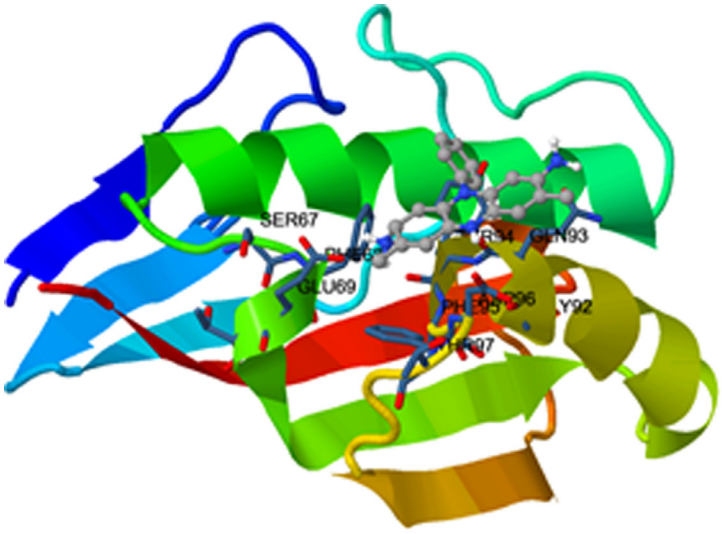

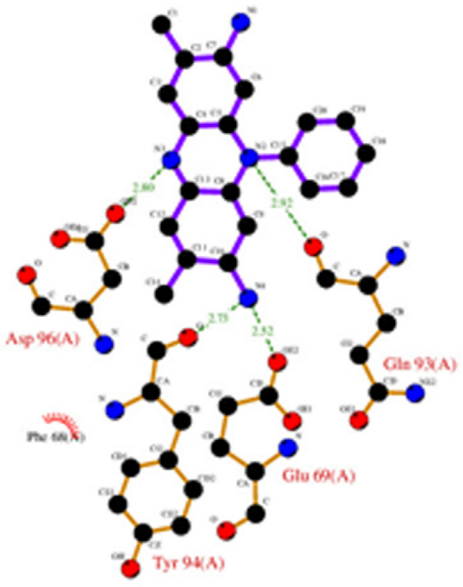

Hydrogen Bonds	Polar	Pi-Pi
N4– GLU69	H15– GLU69	C18– TYR94
N2– GLN93	H16– GLU69	C19– TYR94
N4– TYR94	H17– GLU69	
N3– ASP96	H11– ASP96	

Est. Free Energy of Binding	Est. Inhibition Constant, Ki	vdW + Hbond + desolv Energy	Electrostatic Energy	Total Intermolec. Energy	Interact. Surface
-6.22 kcal/mol	27.75 uM	-4.34 kcal/mol	-2.84 kcal/mol	-7.18 kcal/mol	499.307

Fig. 11. Docking score of ligand and target protein.

4. Conclusion

In current study, Safranin O dye was removed from water samples using the biosorbent *Bacillus subtilis*. The accuracy of the performed biosorption was proven by FT-IR, EDX, SEM and XRD analyzes. The biosorption of Safranin O dye has been carried out at the optimum condition such as pH 5.5–6.5, biosorbent dosage 50 $mg.L^{-1}$ and equilibration time. Furthermore, the biosorption equilibrium data was best fitted to the Langmuir model as compared to Freundlich model, while the D-R model explain the chemisorption nature of biosorption process. Kinetic study showed that the biosorption removal of Safranin O dye was followed by pseudo second order kinetic model very well with good correlation coefficient (R^2=0.94). In addition thermodynamic parameters shows that the biosorption process is spontaneous and endothermic in nature. The computational studies showed that the ligand, which was examined by molecular docking study, exhibited antibacterial properties and had a high activity.

Declaration of Competing Interest

The authors declare that they have no known competing financial interests or personal relationships that could have appeared to influence the work reported in this paper.

CRediT authorship contribution statement

Serap Çetinkaya: Conceptualization, Methodology, Investigation, Writing – original draft. **Savaş Kaya:** Data curation, Writing – review & editing. **Aysun Aksu:** Resources, Investigation. **Halil İbrahim Çetintaş:** Writing – review & editing. **Nida Shams Jalbani:** Methodology, Writing – original draft. **Sultan Erkan:** Writing – review & editing. **Riadh Marzouki:** Funding acquisition, Project administration.

Data Availability

No data was used for the research described in the article.

Acknowledgement

The authors extend their appreciation to the Deanship of Scientific Research at King Khalid University for funding this work through research group under grant number R.G.P.2./224/43.

References

[1] R. Junejo, N. Shams Jalbani, S. Kaya, G. Serdaroglu, S. Şimşek, S. Memon, Experimental and DFT modeling studies for the adsorptive removal of reactive dyes from wastewater, Sep. Sci. Technol. 57 (2022) 339–353, doi:10.1080/01496395.2021.1900252.

[2] P. Kaushik, A. Malik, Fungal dye decolorization: recent advances and future potential, Environ. Int. 35 (2009) 127–141, doi:10.1016/j.envint.2008.05.010.

[3] R. Junejo, N. Shams Jalbani, S. Kaya, S. Erkan, R. Marzouki, S. Memon, Equilibrium and computational chemical modelling studies for the removal of methyl orange and methyl red dyes from water using modified silica resin, Int. J. Environ. Anal. Chem. (2021) 1–17, doi:10.1080/03067319.2021.1979534.

[4] C.A. Fewson, Biodegradation of xenobiotic and other persistent compounds: the causes of recalcitrance, Trends Biotechnol. 6 (1998) 148–153, doi:10.1016/0167-7799(88)90084-4.

[5] A. Srinivasan, T. Viraraghavan, Decolorization of dye wastewaters by biosorbents: a review, J. Environ. Manage. 91 (2010) 1915–1929, doi:10.1016/j.jenvman.2010.05.003.

[6] I.M. Banat, P. Nigam, D. Singh, R. Merchant, Microbial decolorization of textile dye containing effluents: a review, Bioresour. Technol. 58 (1996) 217–227, doi:10.1016/S0960-8524(96)00113-7.

[7] M. Naushad, T. Ahamad, Z.A. AlOthman, H. Ala'a, Green and eco-friendly nanocomposite for the removal of toxic Hg(II) metal ion from aqueous environment: adsorption kinetics & isotherm modelling, J. Mol. Liq. 279 (2019) 1–8, doi:10.1016/j.molliq.2019.01.090.

[8] S. Biswas, P. Basak, Biosorption of the Industrial Dye Remazol Brilliant Blue R by *Bacillus rigiliprofundi*, Microbiology 90 (2021) 816–828, doi:10.1134/S0026261721090010.

[9] M.-.H. Song, S.W. Won, Y.S. Yun, Decarboxylated polyethyleniminemodified bacterial biosorbent for Ru biosorption from Ru-bearing acetic acid wastewater, Chem. Eng. J. 230 (2013) 303e307, doi:10.1016/j.cej.2013.06.087.

[10] A. Bhatnagar, M. Sillanpää, Utilization of agro-industrial and municipal waste materials as potential adsorbents for water treatmentd A review, Chem. Eng. J. 157 (2010) 277–296, doi:10.1016/j.cej.2010.01.007.

[11] S.Y. Kim, M.R. Jin, C.H. Chung, Y.-.S. Yun, K.Y. Jahng, K.-.Y. Yu, Biosorption of cationic basic dye and cadmium by the novel biosorbent *Bacillus catenulatus* JB-022 strain, J. Biosci. Bioeng. 119 (2015) 433–439, doi:10.1016/j.jbiosc.2014.09.022.

[12] B. Volesky, Biosorption and me, Water Res. 41 (2007) 4017–4029, doi:10.1016/j.watres.2007.05.062.

[13] M.M. Areco, S. Hanela, J. Duran, M. dos Santos Afonso, Biosorption of Cu(II), Zn(II), Cd(II) and Pb(II) by dead biomasses of green alga Ulva lactuca and the development of a sustainable matrix for adsorption implementation, J. Hazard. Mater 213-214 (2012) 123–132, doi:10.1016/j.jhazmat.2012.01.073.

[14] N. Masoudzadeh, F. Zakeri, T.b. Lotfabad, H. Sharafi, F. Masoomi, H.S. Zahiri, G. Ahmadian, K.A. Noghabi, Biosorption of cadmium by Brevundimonas sp. ZF12 strain, a novel biosorbent isolated from hot-spring waters in high background radiation areas, J. Hazard. Mater. 197 (2011) 190–198, doi:10.1016/j.jhazmat.2011.09.075.

[15] A. van der Wal, W. Norde, A.J.B. Zehnder, J. Lyklema, Determination of the total charge in the cell walls of gram-positive bacteria, Colloids Surf. B 9 (1997) 81–100, doi:10.1016/S0927-7765(96)01340-9.

[16] Y.-g. Liu, L. Ting, Z.-b. He, T.-t. Li, W. Hui, X.-j. Hu, Y.-m. Guo, H. Yuan, Biosorption of copper (II) from aqueous solution by *Bacillus subtilis* cells immobilized into chitosan beads, Trans. Nonferrous Met. Soc. China 23 (2013) 804–1814, doi:10.1016/S1003-6326(13)62664-3.

[17] B. Tural, E. Ertaş, B. Enez, S.A. Fincan, S. Tural, Preparation and characterization of a novel magnetic biosorbent functionalized with biomass of Bacillus Subtilis: kinetic and isotherm studies of biosorption processes in the removal of Methylene Blue, J. Environ. Chem. Eng. 5 (2017) 4795–4802, doi:10.1016/j.jece.2017.09.019.

[18] V. Chandane, V. Singh, Adsorption of safranin dye from aqueous solutions using a low-cost agro-waste material soybean hull, Desalin. Water Treat. 57 (2014) 1–13, doi:10.1080/19443994.2014.991758.

[19] E. Yavuz, E. Gunes, C. Bulut, Ş. Harsa, A.F. Yenidünya, RFLP of 16S-ITS rDNA region to differentiate Lactobacilli at species level, World J. Microbiol. Biotech. 20 (2004) 535–537, doi:10.1023/B:WIBI.0000043151.09366.d7.

[20] S. UshaNandhini, S. Sudha, J.V. Anusha, S. Manisha, Isolation, identification and extraction of antimicrobial compounds produced by Streptomyces sps from terrestrial soil, Biocatal. Agric. Biotechnol. 5 (2018) 317–321, doi:10.1016/j.bcab.2018.06.024.

[21] A. Klindworth, E. Pruesse, T. Schweer, J. Peplles, C. Quast, M. Horn, F.O. Glökner, Evaluation of general 16S ribosomal RNA gene PCR primers for classical and next-generation sequencing-based diversity studies, Nucleic. Acids Res. 41 (2013) e1, doi:10.1093/nar/gks808.

[22] D. Lunt, HotSHOT DNA extraction. protocols.io (2017).

[23] C. Camacho, G. Coulouris, V. Avagyan, N. Ma, J. Papadopoulos, K. Bealer, T.L. Madden, BLAST plus: architecture and applications, BMC Bioinf. 10 (2009) 421, doi:10.1186/1471-2105-10-421.

[24] K. Katoh, G. Asimenos, H. Toh, Multiple alignment of DNA sequences with MAFFT, Methods Mol. Biol. 537 (2009) 39–64, doi:10.1007/978-1-59745-251-9-3.

[25] M. Kimura, A simple method for estimating evolutionary rates of base substitutions through comparative studies of nucleotide sequences, J. Mol. Evol. 16 (1980) 111–120, doi:10.1007/BF01731581.

[26] K. Tamura, G. Stecher, D. Peterson, A. Filipski, S. Kumar, MEGA6: molecular evolutionary genetics analysis version 6.0, Mol. Biol. Evol. 30 (2013) 2725–2729, doi:10.1093/molbev/mst197.

[27] F. Colak, N. Atar, D. Yazıcıoglu, A. Olgun, Biosorption of lead from aqueous solutions by Bacillus strains possessing heavy-metal resistance, Chem. Eng. J. 173 (2011) 422–428, doi:10.1016/j.cej.2011.07.084.

[28] Z. Bikadi, E. Hazai, Application of the PM6 semi-empiricalmethod to modeling proteins enhances docking accuracy of Auto-Dock, J. Cheminform. 1 (2009) 15, doi:10.1186/1758-2946-1-15.

[29] R. Huey, G.M. Morris, A.J. Olson, D.S. Goodsell, A semiempirical free energy force field with charge-based desolvation, J. Comput. Chem. 28 (2007) 1145–1152, doi:10.1002/jcc.20634.

[30] M. Wakkel, B. Khiari, F. Zagrouba, Basic red 2 and methyl violet adsorption by date pits: adsorbent characterization, optimization by RSM and CCD, equilibrium and kinetic studies, Environ. Sci. Pollut. Res. 26 (2019) 18942–18960, doi:10.1007/s11356-018-2192-y.

[31] Y. Ji, X. Yang, Z. Ji, L. Zhu, N. Ma, D. Chen, X. Jia, J. Tang, Y. Cao, DFT-calculated IR spectrum amide I, II, and III band contributions of N-methylacetamide fine components, ACS Omega 5 (2020) 8572–8578, doi:10.1021/acsomega.9b04421.

[32] A.M. Melin, A. Perromat, G. Déléris, Pharmacologic application of Fourier transform IR spectroscopy: *in vivo* toxicity of carbon tetrachloride on rat liver, Biopolym. Orig. Res. Biomolecules 57 (2000) 60–168 10.1002/(SICI)1097-0282(2000)57:3<160::AID–BIP4>3.0.CO;2-1.

[33] M. Jackson, B. Ramjiawan, M. Hewko, H.H. Mantsch, Infrared microscopic functional group mapping and spectral clustering analysis of hypercholesterolemic rabbit liver, Cell Mol. Biol. 44 (1998) 89–98.

[34] V. Ricciardi, M. Portaccio, L. Manti, M. Lepore, An FTIR microspectroscopy ratiometric approach for monitoring X-ray irradiation effects on SH-SY5Y human neuroblastoma cells, Appl. Sci. 10 (2020) 2974, doi:10.3390/app10082974.

[35] M.K. Sahu, R.K. Patel, Removal of safranin-O dye from aqueous solution using modified red mud: kinetics and equilibrium studies, RSC Adv. 5 (2015) 78491–78501, doi:10.1039/C5RA15780C.

[36] J. Cheriaa, M. Khaireddine, M. Rouabhia, A. Bakhrouf, Removal of triphenylmethane dyes by bacterial consortium, Scientific World J. 512454 (2012) 9, doi:10.1100/2012/512454.

[37] M.K. Sahu, U.K. Sahu, R.K. Patel, Adsorption of safranin-O dye on CO 2 neutralized activated red mud waste: process modelling, analysis and optimization using statistical design, RSC Adv. 5 (2015) 42294–42304, doi:10.1039/C5RA03777H.

[38] G. Upendar, S. Dutta, P. Bhattacharya, A. Dutta, Bioremediation of methylene blue dye using *Bacillus subtilis* MTCC 441, Water Sci. Technol. 75 (2017) 1572–1583, doi:10.2166/wst.2017.031.

[39] A. Dadrasnia, K.S. Chuan Wei, N. Shahsavari, M.S. Azirun, S. Ismail, Biosorption potential of *Bacillus salmalaya* strain 139SI for removal of Cr (VI) from aqueous solution, Int. J. Environ. Res. Public Health 12 (2015) 15321–15338, doi:10.3390/ijerph121214985.

[40] S. Bag, M. Hasan, D. Halder, A. Ghosh, Biosorption of organic dye Acridine orange from aqueous solution using dry biomass of *Bacillus cereus* M116, Arch. Microbiol. 203 (2021) 3811–3823, doi:10.1007/s00203-021-02355-x.

[41] S. Erkan, Activity of the rocuronium molecule and its derivatives: a theoretical Calculation, J. Mol. Struct. 1189 (2019) 257–264, doi:10.1016/j.molstruc.2019.04.042.